Received:Added at production | Revised:Added at production | Accepted: Added at production
DOI: xxx/xxxx

ARTICLE TYPE: Research paper

Engineering Reports

Thermo-economic Assessment of an Integrated Solar Combined Cycle System

Madjid Amani [1] | **Adel Ghenaiet** *[2]|

[1] Laboratory of Mechanical Engineering and Development, National Polytechnic School of Algiers, BP 182 El-Harrach 16200, Algiers Algeria

[2] Laboratory of Energetic Mechanics and Conversion Systems, University of Science and Technology Houari Boumediene, BP32 El-Alia Bab-Ezzouar 16111, Algiers, Algeria

Correspondence
* Adel Ghenaiet,
Laboratory of Energetic Mechanics and Conversion Systems, Faculty of Mechanical Engineering, University of Science and Technology, Houari Boumediene, BP 32 El-Alia, Bab-Ezzouar, 16111, Algiers, Algeria
Email: ag1964@yahoo.com

Funding Information
Project Name: XXXXXXXX
Grant/Award Number: XXXXXXXX

Abstract

The ambitious Algerian program for diversification of electric energy sources is targeting 22 000 MWe from the renewable energy to the horizon of 2030. This study is a thermo-economic assessment of an integrated solar combined cycle system installed in the Saharan region, which during the nights or cloudy days works as a conventional combined cycle and does not need storage or back-up systems. The obtained results show, in one side that the solar electricity ratio may reach about 17 % and the global thermal efficiency up to 63 %, leading to lower fuel consumption and carbon emission. In the other side, the economic assessment depicts that the levelized cost of energy may reach a value of 0.0222 $/kWh which is about 28 % higher than CC plants. By considering the environment this latter is even more and may reach about 0.0272 $/kWh, but the annual solar contribution, relatively to that installation site, allows about 18.45 million $ of fuel saving and avoidance of 0.89 million ton of CO_2 emission over 30 years of operation.

KEYWORDS

Integrated solar combined cycle, Parabolic trough, Heat solar steam generator, Thermo-economic performance, Levelized cost of energy.

1 | INTRODUCTION

The global energy consumption has increased rapidly leading to the global warming as a result of emissions of carbon dioxide (CO_2) and methane into the atmosphere [1] added to the shrinkage in the fossil energy availability. All these made the recourse for an efficient energy conversion and the development of renewable energy ever more critical. The integration of solar energy via the combination of concentrated solar power technology (CSP) with Combined Cycle (CC) has resulted in less capital cost and continuous power supply, in addition to thermal efficiency improvement and CO_2 emission reduction [2]. A number of CSP plants are under development over the world. Typically there are nine large-scale solar power plants of 354 MW installed in the Mojave Desert and several others operating in Italy, Iran and North-Africa.

Received:Added at production | Revised:Added at production | Accepted: Added at production
DOI: xxx/xxxx

One of the systems that will be studied herein is that of Integrated Solar Combined Cycle (ISCC) system incorporating the technology of Parabolic Trough Collectors (PTC), which is the most mature technology among CSPs. Moreover, The ISCC system is one way to deploy CSP with low investment risk while retaining power dispatchability, and subsequently the Thermal Energy Storage (TES) may be eliminated or significantly reduced for a solar hybrid plant [3]. Besides, the integration of TES into ISCC has the advantage to increase the solar share but may induce more cost [4]. In the concept of ISCC the solar heat is introduced in the bottoming Rankine cycle, hence a Heat Solar Steam Generator (HSSG) is added which offers several advantages over the solar-only electric generation system or Rankine cycle [5]. Okoroigwe et al. [6] reviewed CCs coupled with SPT and compared to those using Parabolic Trough Collector (PTC) technology and concluded that the former is still immature. Zhu et al. [3] examined the thermodynamic impact of integrating solar energy into CC plants and concluded that with a thermal solar input of 200 MW into HRSG the output can be boosted from 475 MWe to about 558 MWe, which has a benefit on fuel saving and pollution reduction. With PTC technology the solar energy is transferred to synthetic oil in the absorber tube and then via an intermediate oil-to-water/steam heat exchanger is transmitted into the Rankine cyle, hence resulting in the so-called Heat Transfer Fluid (HTF) technology. Another configuration is the Direct Steam Generation (DSG) used to increase the power output during the sunny periods. Nezammahalleh et al. [7] considered three configurations of ISCC-DSG technology, ISCC-HTF technology and a solar electric generating system (SEGS). As revealed, both ISCC-DSG and ISCC-HTF present a high net efficiency, but ISCC-DSG is the best option due to high temperature of superheated steam produced in the receiver, which is economically viable since no additional investment is required compared when using oil as HTF. Rovira et al. [8] compared ISCC technology using HTF with DSG and showed that the performance of ISCC-DSG is improved compared to HTF that requires an additional steam generator. Another promising technology of concentrating solar energy is the solar tower (ST) which is expected to lead in the future. A comparative study [9] between Solar Rankine Cycle (SRC) and ISCC plants based on PTC/ SPT system and a molten salt to transfer heat to the water loop in SRC and to the synthetic oil (Therminol VP-1) in ISCC showed that, with the same aperture area of the solar field, the coupling with PTC caused low performance since less quantity of solar energy is intercepted compared to heliostat field. Abdel Dayem et al. [10] simulated the Kuraymat (Egypt) ISCC using TRNSYS and compared the predicted thermodynamic performance with the measured data under the same conditions of design specifications and weather, and concluded good agreements. Aldali et al. [11] studied the thermodynamic performance of ISCC system under the Libyan weather where two operation modes (fuel saving and power boosting) with the same solar field area, and concluded a reduction in fuel consumption and CO_2 emission. Dersch et al. [12] found that the integration of PTC technology with CC plant provides an interesting way for solar electricity generation, in addition to the environmental and economic benefits. Montes et al. [13] showed the benefit of coupling the solar field to CC, evidently in a hot dry climate such as in Las-Vegas and Almeria where the good coupling of solar thermal power made ISCC to operate efficiently and the cost of solar electricity gets less. Antonanzas et al. [14] found that the solar hybridization with CC installed through Spain has increased the electricity production in the peak hours as well as the overall thermal efficiency and reduced CO_2 emission. During high ambient temperatures coinciding with the period of higher normal radiation the steam produced by the solar collectors alleviated the drop in electricity production by CC plants during the peak demand periods and improved the overall efficiency.

Besides the thermodynamic study the economic assessment is required from the point of view of viability for electricity production. Various previous techno-economic studies have

Received:Added at production | Revised:Added at production | Accepted: Added at production
DOI: xxx/xxxx

investigated the performance of ISCC technology, where the Levelized Cost of Energy (LCOE) is more appropriate criterion. Price et al. [15] quantified the cost reduction potential of LCOE for different configurations of solar energy integration. A comparative investigation to a reference 50 MW power plant with the solar mode only without a storage has revealed that the substitution by an ISCC may reduce the cost of electricity by 33% (0.11 to 0.073 $/kWh), while the increase of concentrator size from 50 m to 150 m reduces the cost from 0.11 to 0.10 $/kWh. Horn et al. [16] investigated the technical and economical aspects of ISCC installation in Egypt; therefore a comparative study between ISCC using PTC technology and solar tower technology was carried out and allowed to conclude that from the point of view of electricity cost generation and environmental effect PTC is still an attractive technology. Similarly, Hosseini et al. [17] assessed the technical and economic aspects for six different sizes of ISCC power in Iran. Based on LCOE and when the environmental effect is considered, they concluded that ISCC using 67 MW integrated to CC is the best choice for the construction of the first solar power plant in Iran. Also, Mokheimer et al. [18] made a techno-economic comparative study to integrate three types of CSP technologies (PTC, Linear Fresnel Reflector (LFR) and ST) with a conventional GT cogeneration plant of different power 50-150 MW under Dhahran (Saudi Arabia) weather conditions, where THERMOFLEX with PEACE software were used. They concluded that LFR technology is the optimal configuration of solar integration with the steam side of GT cogeneration with 50 MWe output. Duan et al. [19] proposed a novel solar integration with CC (HRSG with two pressure levels) using PTC technology and a part of compressed air from the compressor is used as HTF through the receiver of solar PTC field. This novel ISCC using compressed air has more advantages in terms of performance and economy compared to ISCC using oil as HTF. Li et al. [20] presented a novel integration of solar energy into CC with two different pressure and temperature levels in HRSG using concentrating and non-concentrating solar systems which are PTC using DSG system and Evacuated Tube (ET). These two types of solar-collectors in a temperature cascade are shown to contribute positively in the power plant performance in terms of solar heat conversion, efficiency and lowering LCOE compared to ISCC-DSG system power plant.

The present study concerns the thermodynamic and economic assessments of ISCC power plants integrating an HSSG and using solar thermal energy collected by HTF through PTC without any TES to reduce the cost and to evaluate their operation and efficiency under the Algerian Sahara climate with the solar radiation varying during the day and year. HSSG was chosen to operate as a boiler in parallel to HRSG for enhancing the quantity of steam generated during the sunny periods, thus only an evaporator section is used and subsequently avoids extra preheating and superheating exchangers. As the heat exchangers are the important subsystems, the method of pinch point and approach point are used in the thermodynamic modelling. The obtained results show prospective results and viability of such technology which also may serve to support and guide further installations.

2 | THERMODYNAMIC MODELLING

As shown by Fig.1, this ISCC consists of a solar field via PTC, two GT units and Steam Power Turbine (SPT) fed by two HRSG with a simple pressure level in addition to HSSG working as an evaporator. The solar energy is transferred to HTF (synthetic oil Thermonol VP-1 which has a proven maturity in all solar thermal power plants, of a temperature range of 13 - 395°C limited by the thermal stability [21]) in the absorber tube and via an intermediate oil-to-water/steam heat exchanger is transmitted into the Rankine cycle. During the cloudy periods and nights the power plant operates as a conventional CC, while in the sunny periods one part of feed water is withdrawn from HRSG and converted into saturated steam by HSSG and then

Received:Added at production | Revised:Added at production | Accepted: Added at production
DOI: xxx/xxxx

returned to HRSG where it is mixed and superheated. The supplement of solar thermal energy provides an increase in steam mass flow of the Rankine-Hirn cycle.

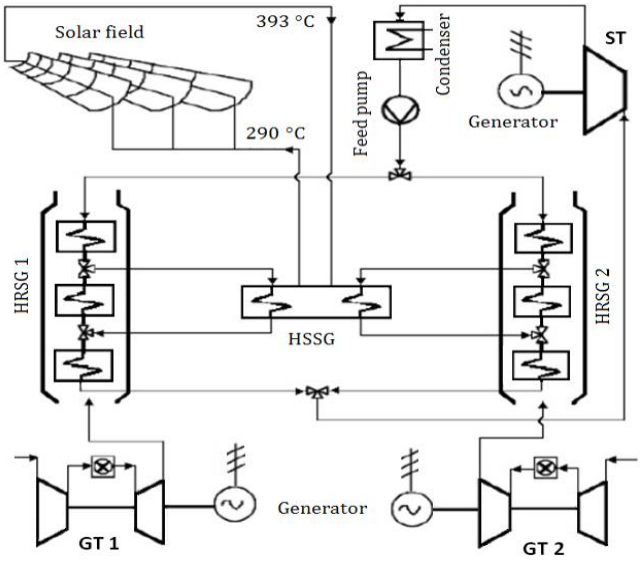

Figure 1. Schematic of ISCC power plant

2.1 Solar field

Accurate radiation data are critical in performance prediction and sizing and selection of CSP equipments, which are obtained from a combination of ground measurements and satellite data [22]. To overcome the difficulty of data availability, the radiation models for direct normal irradiation (DNI) are an alternative recourse, which are simple models requiring less than three inputs such as: Hottel, Liu and Jordan (HLJ) [23], Meinel [24], Kumar [25] and ASHRAE [26], while more inputs are for the complex models: Davies and Hay model [27] and Iqbal [28] etc. The present power plant corresponds to operating conditions in Hassi-R'mel (Algerian Sahara) of latitude of 33.8 deg. The adopted estimate of DNI is that of HLJ [23] model as below, which has been frequently used to assess clear sky solar radiation for numerous locations and among them the Saharan regions.

$$DNI = \tau_b I_{so} \cos\theta_z \tag{1}$$

The solar field parameters and specifications are given in the Tables 1 – 4. To evaluate the thermal performance of solar field the energy balance between solar radiation and heat absorption by HTF and heat losses are estimated. The useful solar energy gained through the absorber of PTC is obtained by an equation due to Zarza [29].

$$Q_{PTC} = A_c DNI \cos\theta\, \eta_{optic} K(\theta) - A_{abs} U_{abs} (T_{abs} - T_{abs}) \tag{2}$$

The incidence angle modifier is given as follow:

$$K(\theta) = 1 - 2.23073\ 10^{-4}(\theta) - 1.1\ 10^{-4}(\theta)^2 - 3.185\ 10^{-6}(\theta)^3 - 4.855\ 10^{-8}(\theta)^4 \tag{3}$$

The absorber temperature is evaluated from:

Received:Added at production | Revised:Added at production | Accepted: Added at production
DOI: xxx/xxxx

$$T_{abs} = \sqrt[4]{\left(\alpha\ DNI\ C_c \frac{\eta_{optic}}{\sigma\varepsilon}\right) + {T_a}^4} \quad (4)$$

The heat loss coefficient depends on the absorber temperature found experimentally by performing specific thermal loss tests with the solar collector operating at several temperatures within its typical working temperature range. The variation of thermal loss coefficient versus the receiver pipe temperature is usually expressed with a second order polynomial equation, with b and c obtained experimentally [29].

$$U_{abs} = a + b\ (T_{abs} - T_a) + c\ (T_{abs} - T_a)^2 \quad (5)$$

The solar field performance is the useful solar energy, HTF mass flow and the solar field efficiency. The total useful energy gained by HTF is given by:

$$Q_{SF} = N_L C_L Q_{PTC} \quad (6)$$

Where C_L, N_L are respectively, the number of collectors in each row and the number of lines in the solar field.

HTF mass flow is given by:

$$\dot{m}_{SF} = \frac{Q_{SF}}{C_{p,HTF}\Delta T_{SF}} \quad (7)$$

The solar field efficiency is the ratio of the net useful energy gained by HTF in the solar field and the total quantity of solar beam reaching the mirrors:

$$\eta_{SF} = \frac{Q_{SF}}{DNI\ A_C N_L C_L} \quad (8)$$

Table 1. Solar collector specifications [30]

Parameters	Values
Aperture area (m2)	545
Concentration ratio	82
Optical efficiency (%)	0.80
Aperture (m)	5.76
Length (m)	99

Table 2. Solar field operation parameters [30]

Parameters	Values
Number of collectors in each row	4
Number of lines	56
HTF inlet temperature (°C)	293
HTF outlet temperature (°C)	393
Solar field area (m2)	183120

Table 3. Collector optical performances [31]

Parameters	Symbols	values	units
Intercept factor	γ	96	%
Absorptivity	α	95	%

Received:Added at production | Revised:Added at production | Accepted: Added at production
DOI: xxx/xxxx

Reflectivity	ρ	98	%
Transmissivity	τ	97	%
Concentration ratio	*Cc*	82	-

Table 4. Site data [32]

Parameters			
Latitude	ϕ	33.8	degree
Ambient temperature	T_a	20	°C
Solar constant	I_{sc}	1367	W/m2
Relative humidity	RH	58	%

2.2 Gas cycle

In currently technology of GT the polytropic efficiency of compressor and turbine are about 0.9 [33], which is considered constant during calculations. The mechanical and electrical efficiency are in-between 97-99 % and of combustion chamber is about 98 % [34]. Typical value of pressure drop in combustion chamber and HRSG are 2 - 6 % [35] and for filtration 0.005 - 0.015 bar [36]. The specific heat of air in compressor and gases in turbine section correspond to polynomial regressions with constants obtained from [37]. The outlet temperatures from compressor and turbine are obtained from isentropic efficiency via polytropic efficiency and pressure ratio/ expansion ratio.
The work of the turbine is summed from works of expansion gases and cooling air [33], [34], [38]. The net power of GT is the difference between that produced by the turbine and consumed by the compressor.

$$P_{GT} = \eta_e \eta_m \dot{m}_a \left[(1 + f + e)\overline{C_{pg}}(T_{g3} - T_{g4}) - \frac{1}{\eta_m}\overline{C_{pa}}(T_{a2} - T_{a1})\right] \quad (9)$$

The thermal efficiency given by.

$$\eta_{GT} = \frac{P_{GT}/\dot{m}_a}{f\ Lcv} \quad (11)$$

The fuel (natural gas) mass flow rate is obtained from the energy balance applied to the combustion chamber and subsequently the fuel by air ratio:

$$f = \frac{\dot{m}_f}{\dot{m}_a} = \frac{C_{pg}T_{g3} - C_{pa}T_{a2}}{\eta_b Lcv - C_{pg}T_{g3}} \quad (12)$$

The thermodynamic model is validated upon Siemens SGT 800 of 47 MW which is the main part of Hassi R'mel's power plant. Its main data are summarized in Table 5. Table 6 depicts good agreements for the produced power, thermal efficiency, exhaust gases flow rate and temperature.

Table 5. GT data

Parameters	Symbols	Values
Ambient conditions	T_a , P_a	21°C, 1.013 bar

Received:Added at production | Revised:Added at production | Accepted: Added at production
DOI: xxx/xxxx

Turbine inlet temperature	T_{g3}	1200 °C
Compressor Pressure ratio	π_C	19.9
Turbine blade temperature	T_b	850 °C
Cooling effectiveness	ε_{cool}	42 %
Compressor polytropic efficiency	η_{pC}	90 %
Turbine polytropic efficiency	η_{pT}	91 %
Combustion efficiency	η_b	98 %
Mechanical efficiency	η_m	98 %
Electrical efficiency	η_e	98.5 %
Compressor inlet pressure loss	δP_{in}	0.5 %
Combustion pressure loss	δP_b	2 %
Pressure losses in HRSG	δP_{HRSG}	2.5 %
Natural gas heat calorific value	Lcv	46595 kJ/kg
Output	P_{GT}	30 MW

Table 6. GT validation

Parameters	SGT-800	Predicted	Error (%)
Compressor air mass flow (kg/s)	129	124.2	3.7
Exhaust gases mass flow (kg/s)	131.5	126.8	3.5
Exhaust gases temperature (°C)	544	542	0.3
Gas turbine efficiency (%)	37.5	37.86	0.9

2.3 Steam cycle

The steam pressure and the pinch point play a crucial role in determining the gas–steam temperature profiles. The pinch and approach points are selected. Moreover, the exit gas temperature from the economizer cannot be arbitrarily assumed [39]. These temperature profiles serve to evaluate the steam generation since the principle inputs to HRSG are the gas temperature outlet (T_{g4}) and the mass flow ($\dot{m}_g$). With the solar radiation varying during the day, the exhaust gas flow rate/ temperature conditions to the steam are evaluated iteratively. A subprogram is used to interpolate between the tabulated values of enthalpy and entropy for water/steam at each point including the steam quality x. The temperature profiles shown in Fig. 2 are determined based on the data given in Table 7 and the definitions of pinch point $\Delta Tpp = T_{g5'} - T_{sat}$ and approach point $\Delta Tap = T_{sat} - T_{w7}$.

Table 7. Pinch and approach points [39]

Evaporator type	Plain tubes	Finned tubes	For both
gas inlet temp (°C)	pinch point (°C)	pinch point (°C)	approach point (°C)
650-900	60-85	20-35	20-40
375-650	40-60	5-20	5-20

Received:Added at production | Revised:Added at production | Accepted: Added at production
DOI: xxx/xxxx

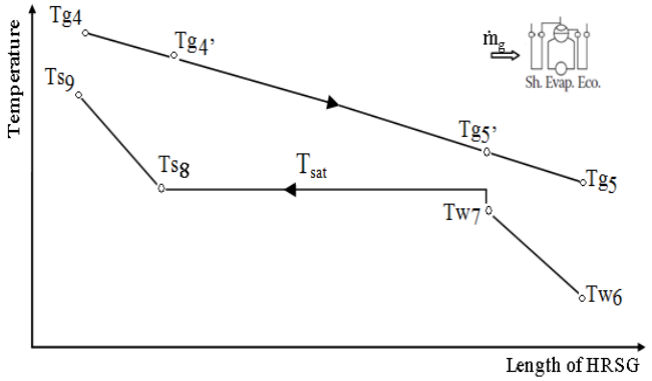

Figure 2. Gas-steam temperatures profiles

ISCCS plant consists of two HRSG, thus the target amount of steam is the double. The determination of the steam generated during nights or cloudy periods follows the balance of the superheater and evaporator. The selected parameters are from Table 8 and the obtained performances are listed in Table 9.

$$\dot{m}_g \bar{C}_{pg}\left(T_{g4} - T_{g5'}\right) = \dot{m}_s(h_{s9} - h_{sat}) \tag{13}$$

With $T_{g5'} = T_{sat} + T_{pp}$

$$\dot{m}_s = \frac{\dot{m}_g\ \bar{C}_{pg}\ (T_{g4} - T_{g5'})}{(h_{s9} - h_{sat})} \tag{14}$$

Energy balance of the economizer

$$T_{g5} = T_{g5'} - \frac{\dot{m}_s(h_{w7} - h_{w6})}{\dot{m}_g \bar{C}_{pg}} \tag{15}$$

Table 8. HRSG parameters

$\dot{m}_g$(kg/s)	*Tg4* (°C)	*Tw6* (°C)	*ΔTpp* (°C)	*ΔTap* (°C)	*Ts9* (°C)	*Pfb* (bar)
126	542	45	11	8	500	93

Table 9. HRSG performance

Surface	Gas temp in/out (°C)	Wat /Stm in /out (°C)	Duty (MW)	Press (bar)	Mass flow (kg/s)	Pinch (°C)	Approach (°C)	*UA* (kW/°C)
Sh	542 / 473	305.7 / 500	10.97	93	16	-	-	120.54
Evap	473 / 316	297.7 /305.7	25.33	93	16	11	8	370.17
Eco	316 / 205	45 / 297.7	18	93	16	-	-	272.22

It is required to predict the performance of the heat exchangers network HRSG and HSSG during sunny days while the solar radiation varies. In these calculations several initial values were guessed before arriving iteratively at the final heat balance and the duty added to the steam generation. The design value of $(UA)_d$ is corrected by using appropriate factors for gas properties and heat balance of each section. First, the temperature correction factor F which reflects gas properties for each surface is computed, and then the transferred heat using the expression:

$$Q = (UA)\ F\ \Delta TLM \tag{17}$$

The steam flow rate $\dot{m}_s$ is assumed at first, and then iterations are required to arrive at the final value. The reference value of (UA) is obtained from the duty Q and logarithmic mean

Received:Added at production | Revised:Added at production | Accepted: Added at production
DOI: xxx/xxxx

temperature difference ΔTLM and the correction factor F for each surface of the heat exchangers network such as superheater, evaporator, and economizer:

$$(UA)_d = \left(\frac{Q}{F\Delta TLM}\right)_d \tag{18}$$

The update of (UA) is obtained using correction factors for gas flow and steam flow. The steam flow correction is not required for evaporator and economizer [40].

$$UA = (UA)_d \left(\frac{\dot{m}_g}{\dot{m}_{gd}}\right)^{0.65} \left(\frac{F}{F_d}\right) \left(\frac{\dot{m}_s}{\dot{m}_{sd}}\right)^{0.15} \tag{19}$$

2.4 Determination of steam generation

The determination of steam generated during nights or cloudy periods follows the energy balance of the superheater and evaporator. As first solar beam appears the plant works as ISCC and the amount of steam generated is the double Since ISCCS plants consists of two HRSG. To recover some heat from the solar filed a solar steam generator HSSG is used, made up of one heat exchanger: evaporator section. Referring to Rankine-Hirn cycle (Fig. 3), the steam mass flow generated during the day is evaluated as follows:

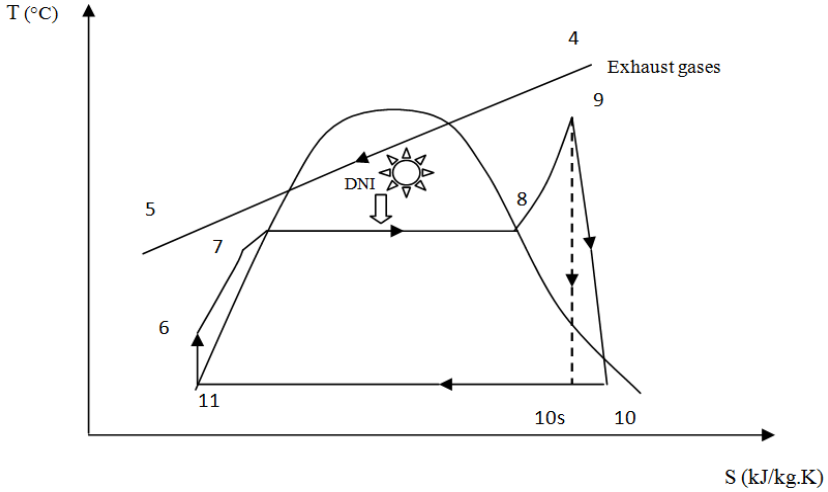

Figure 3. Rankine-Hirn cycle

It is assumed that the water feed pump outlet pressure is equal to P_{FP} = 93 bars [30]. The input data are summarized in Table 10.

The first value of steam mass flow is assumed:

a- Super heater level

Assume T_{s9}

then calculate $Q_a = \dot{m}`_s(h_{s9} - h_{sat})$ and $T_{g4,} = T_{g4} - \frac{Q_a}{\dot{m}_g C_{pg}}$

Calculate $Q_t = (UA)F\Delta TLM$ and $\Delta TLM = \frac{\left(T_{g4'} - T_{sat}\right) - (T_{g4} - T_{s9})}{ln\frac{(T_{g4'} - T_{sat})}{(T_{g4} - T_{s9})}}$

Estimate $(UA) = (UA)_d \left(\frac{\dot{m}_g}{\dot{m}_g}\right)^{0.65} \left(\frac{F_g}{F_{gd}}\right) \left(\frac{\dot{m}`_s}{\dot{m}_{sd}}\right)^{0.15}$

Check: $\frac{(Q_a - Q_t)}{Q_a} < \varepsilon$

Received:Added at production | Revised:Added at production | Accepted: Added at production
DOI: xxx/xxxx

Then put $Q_t = Q_1$ and pass to the second step which is the evaporator level. If the assumed duty does not match the exhaust gases to the steam at the superheater level, the case $\frac{(Q_a - Q_t)}{Q_a} \geq \varepsilon$, another value of T_{s9} is assumed and the superheater calculations are repeated.

b) Evaporator level

$$ln\frac{(T_{g4\prime} - T_{sat})}{(T_{g5\prime} - T_{sat})} = \frac{UA}{\dot{m}_g C_{pg}}$$

and $$ln\frac{(T_{g4\prime} - T_{sat})}{(T_{g5\prime} - T_{sat})} = K(\dot{m}_g)_d^{-0.4}$$

with $K = f(A/C_{pg})$ $K = (\dot{m}_g)_d^{0.4} ln\frac{(T_{g4\prime} - T_{sat})}{(T_{g5\prime} - T_{sat})}$

Then calculate $T_{g5\prime}$ from:

$$ln\frac{(T_{g4\prime} - T_{sat})}{(T_{g5\prime} - T_{sat})} = K(\dot{m}_g)^{-0.4}$$

then $Q = \dot{m}_g C_{pg}(T_{g4\prime} - T_{g5\prime})$

$Q_2 = Q + \frac{Q_{SF}}{2}$ and $Q_2 = \dot{m}`_s(h_{sat} - h_{w7})$

$\frac{Q_{SF}}{2}$ is the solar energy carried by HTF and released to HSSG.

c) Economizer level

Assume T_{w7}:

$Q_a = \dot{m}`_s(h_{w7} - h_{w6})$

and $T_{g5} = T_{g5\prime} - \frac{Q_a}{\dot{m}_g C_{pg}}$

$Q_t = (UA)F\Delta TLM$

With: $(UA) = (UA)_d \left(\frac{\dot{m}_g}{\dot{m}_{gd}}\right)^{0.65} \left(\frac{F}{F_d}\right)$

and $\Delta TLM = \frac{(T_{g5\prime} - T_{w7}) - (T_{g5} - T_{w6})}{ln\frac{(T_{g5\prime} - T_{w7})}{(T_{g5} - T_{w6})}}$

If the assumed duty does not match the exhaust gases to steam at economizer level, case $\frac{(Q_a - Q_t)}{Q_a} \geq \varepsilon$ assume another value of T_{w7} and repeat the economizer calculations by $Q_3 = Q_t$

Calculation of the steam mass $\dot{m}_s = \frac{(Q_1 + Q_2 + Q_3)}{(h_{s9} - h_{w6})}$, and then check: $\frac{(\dot{m}`_s - \dot{m}_s)}{\dot{m}`_s} < \varepsilon$. If the assumed steam mass flow value $\dot{m}_s$ does not match, the case $\frac{(\dot{m}`_s - \dot{m}_s)}{\dot{m}`_s} \geq \varepsilon$, the calculated steam mass flow rate is reassigned as a value and computations starts from the first step which is the superheater and the whole calculation procedure is repeated.

Table 10. Data to steam cycle

Parameters	Symbols	Values
Ambient temperature and pressure	T_a & P_a	20°C and 1.013 bar
HRSG steam outlet temperature at design mode	T_{w9d}	500 °C
HRSG water inlet temperature	T_{w6}	45 °C
water feed pump outlet pressure	P_{FP}	93 bar
Steam turbine mechanical efficiency	η_m	98 %
Steam turbine electrical generator efficiency	η_e	98 %

Received:Added at production | Revised:Added at production | Accepted: Added at production
DOI: xxx/xxxx

The mechanical work of steam is converted to electrical energy by a generator.

$$P_{STP} = \eta_m \eta_e (P_{SPT} - W_{FP}) \tag{20}$$

The plant net output is summed from GT and SPT outputs.

$$P_{ISCC} = 2\, P_{GT} + P_{SPT} \tag{21}$$

The power plant efficiency is calculated as the net energy produced divided by the total thermal energy provided from fuel:

$$\eta_{ISCC} = \frac{P_{ISCC}}{\dot{m}_f L_{cv}} \tag{22}$$

And the specific fuel consumption of the power plant:

$$sfc = \frac{3600\, \dot{m}_f}{P_{ISCC}} \tag{23}$$

The net solar electricity is the difference of the plant output between sunny and night periods. With P_{cc} is the plant output during nights while it operates as a CC. Therefore solar electric ratio is given as follow:

$$Sol, elec, rat = 1 - \frac{P_{CC}}{P_{ISCC}} \tag{24}$$

3 | ECONOMIC ASSESSMENT

The economic assessment of GT, CC and ISCC power plant considers *LCOE* to compare between them. The economic lifetime of steam power plant and ISCC are expected to reach 30 years [18], while the GT life expectancy is about 15 years, after which the replacement cost has to be considered for both ISCC and CC [17], [20]. The conventional CC is taken as the reference power plant for the purpose of comparison. The economical assumptions and data for this economic analysis are presented in Table 11.
The investor has to calculate LCOE of power plant before starting the investment which is given in the units of currency (US dollar) per kilowatt-hour ($/kWh), and calculated according to reference [16], [17] and [20].

$$LCOE = \frac{(CRF.C + O\&M + PVF)}{Pel\_an} \tag{25}$$

$$CRF = \frac{R}{(1 - (1+R)^{-N})} \tag{26}$$

C : Capital cost
CRF : Cost recovery factor
O&M : Operation and maintenance
PVF : Annual fuel cost
Pel_an: Annual electrical energy production
R : Discount rate
N : Expected life time of power plant (Year)

Received:Added at production | Revised:Added at production | Accepted: Added at production
DOI: xxx/xxxx

The total investment cost for ISCC is the sum of GT, ST and solar units' costs. The operation and maintenance costs (O&M) include labour, spare-parts and consumables. The normal maintenance equipment is estimated [17] as follows**:**

$$O\&M = k_{sol}C_{sol} + k_sC_s + k_gC_g \quad (27)$$

Table 11. Assumptions and data [16], [17], [41]

Assumptions and data	Value
Life expectancy of solar field (year)	30
Life expectancy of steam unit (year)	30
Life expectancy of gas unit (year)	15
Annual discount rate R (year)	10
Capacity factor	0.8
Direct costs	
Specific cost of solar field $_{sol}$($/kW)	1400
Specific cost of steam unit C_s($/kW)	635
Specific cost of gas unit C_g ($/kW)	235
Contingency (% of direct costs)	10
Indirect costs	
Engineering, procurement and construction (% of direct costs)	13
O&M cost factor of solar field k_{sol}(%)	1.5
O&M cost factor of steam unit of CC k_s(%)	2
O&M cost factor of gas unit k_g(%)	5
L_{cv} (kJ/kg)	46595.3
Fuel price ($/MMBTU) based on average 2018	3.16
Emissions ($/ton)	9.9

4 | RESULTS AND DISCUSSION

The on-site (Hassi R'mel, Algeria) the average day temperature during 21$_{st}$ of March is equal to 20°C [32] which corresponds to the design conditions and selected as the reference day in the present study. The solar field subprogram calculates the supplied solar energy to HSSG, which according to Fig. 6 illustrates the variation of *DNI* during the day and shows that at midday its maximum reaches a value of 770 W/m2. Fig. 7 represents the subsequent solar thermal output during the day as it varies with the solar radiation from sunrise until sunset.

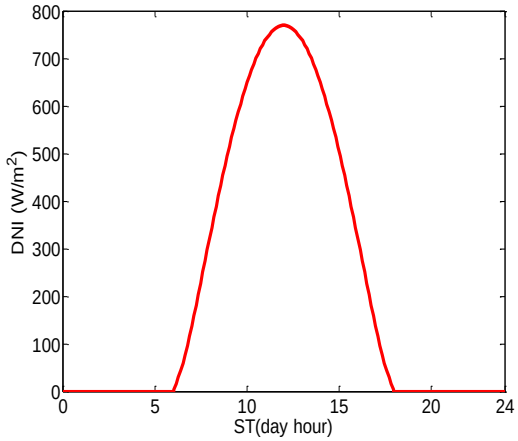

igure 4. Variation of DNI

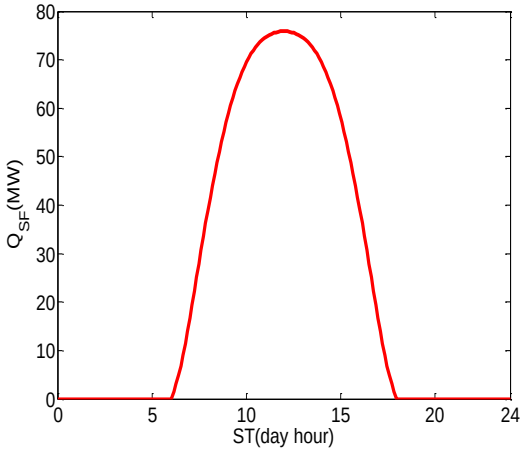

Figure 5. Solar Field output

Received:Added at production | Revised:Added at production | Accepted: Added at production
DOI: xxx/xxxx

As shown in Fig. 6(a), the additional steam mass flow generated by HSSG varies as it depends on solar radiation to reach a maximum of 65 kg/s when DNI gets at maximum. As a result, the total SPT output (Fig. 6(b)) is equal to 62 MW compared to that at night equal to 35 MW, which means an increase in electricity production about 27 MW. Fig. 6(c) gives an idea about the power plant output during the 21st of March (design point) at the specified site conditions. During the nights or cloudy periods ISCC operates as CC and produces about 129 MW and its thermal efficiency reaches 52 %, according to Fig. 6(d), while during the day, the net electricity production is increased to 156 MW and the thermal efficiency reach its highest value of 63 % at midday. The estimated solar electricity ratio **(**Fig. 6(e)**)** based on the difference in electrical output of ISSC mode and CC mode varies from sunrise to sunset according with solar radiation to reach a maximum of 17 % at midday.

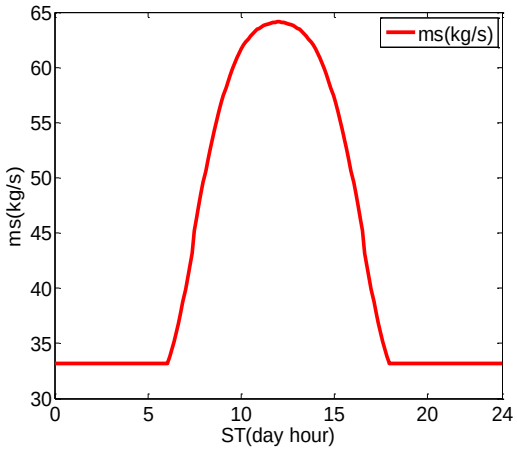

(a)

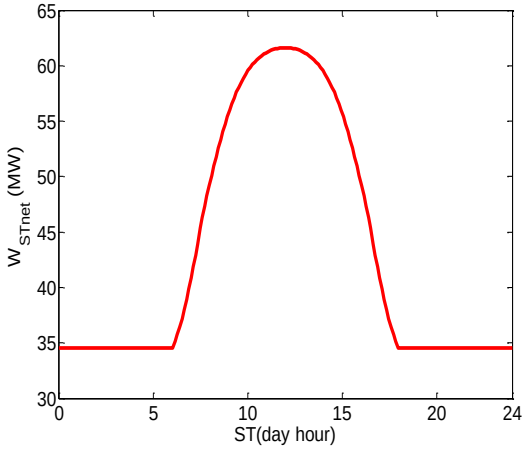

(b)

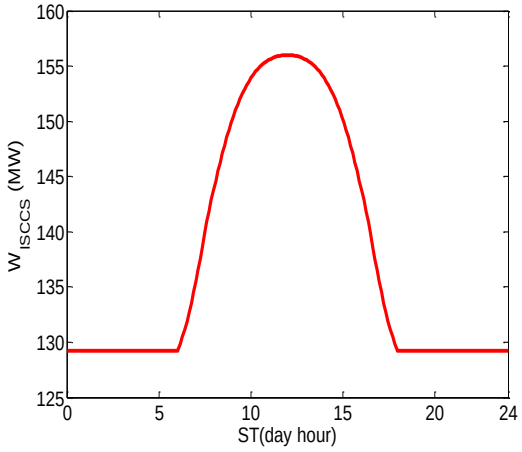

(c)

Received:Added at production | Revised:Added at production | Accepted: Added at production
DOI: xxx/xxxx

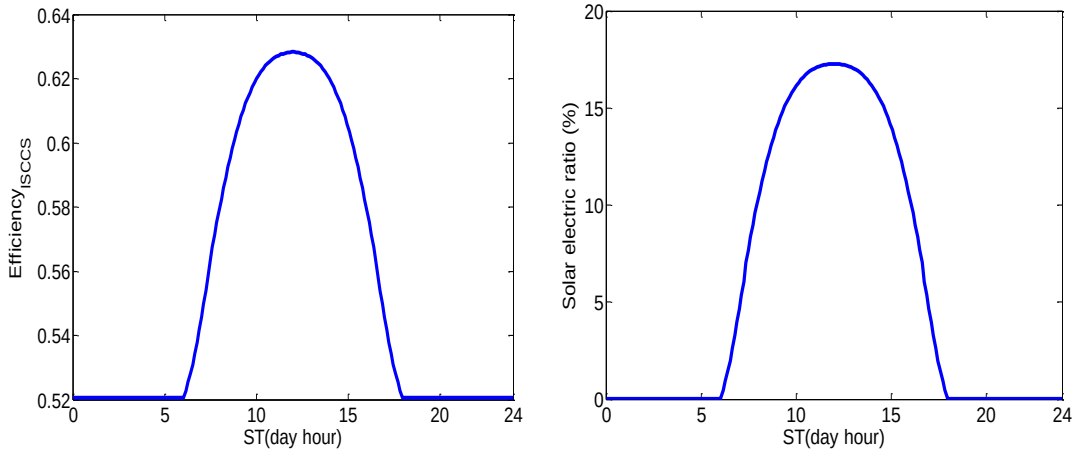

(d) **(e)**

Figure 6. Computed performance: a) Steam generated; b) Steam power turbine output; c) ISCC output; d) ISCC efficiency; e) Solar electric ratio

In order to estimate the sensitivity of ISCC power plant vis-à-vis the ambient temperature through the whole year; the average ambient temperature of each month (Table 12) is introduced. Also, the values of DNI were evaluated for monthly periods based on the daily average values which were averaged over one month. The obtained results are shown in Fig. 7 based on monthly average ambient temperatures during days. As shown, the output and thermal efficiency of ISCC plant exhibit a drop as the ambient temperature gets to its highest value. If the plant works as a conventional CC there is a significant drop in the output around 1 MW compared to ISCC and this is explained by the negative impact of high ambient temperature on GT. The slight decrease in performance of ISCC in hot periods is explained by the advantage of converting solar energy in producing additional steam in HSSG. Fig. 7(a) and Fig. 7(b) reveal that the additional steam generated by coupling the CC with the solar field compensates for the loss in power during the hot days, and hence the solar integration with CC is a good solution. It can be concluded that during high ambient temperatures coinciding with the period of higher normal radiation, the steam produced by the solar collectors alleviated the drop in electricity production by CC plants during the peak demand periods and improved the overall efficiency. Fig. 7(c) displays the impact of ambient temperature on the produced electricity by the solar field as quantified by the solar electric ratio which seems decreasing slightly with the ambient temperature such as the case during the summer.
Fig. 8 displays the response of ISCC plant to the variation in the ambient temperature during nights or cloudy periods depicted in Table 13. As shown the power output drops significantly from cold to hot periods such as in summer. Since ISCC works as CC and due to negative impact of ambient temperature the power drops for about 1 MW (Fig. 8(a)) as well as the thermal efficiency about 0.3 % as depicted in Fig. 8(b).

Table 12. Average ambient temperatures during the day [32]

Month	Jan	Feb	Mar	Apr	May	Jun	Jul	Aug	Sep	Oct	Nov	Dec
T(°C)	15.9	18.0	19.1	27.1	31.4	34.3	40.2	40.0	35.3	28.9	21.3	14.4

Received:Added at production | Revised:Added at production | Accepted: Added at production
DOI: xxx/xxxx

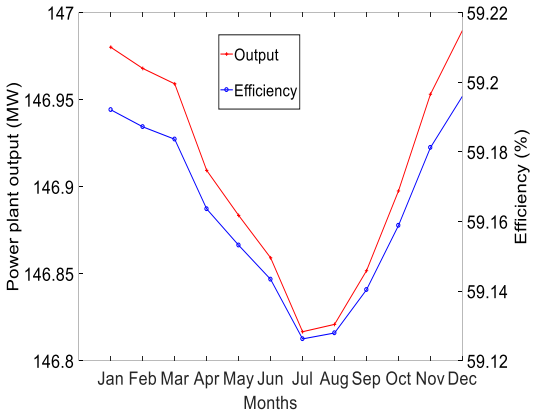

(a)

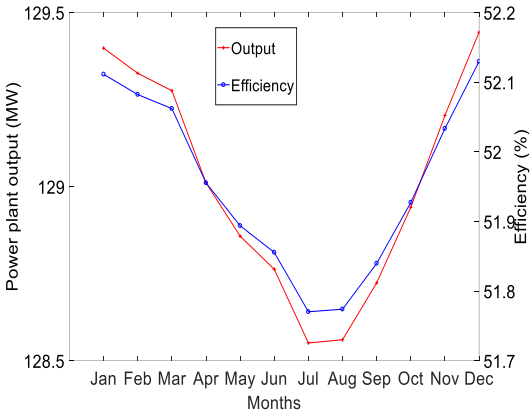

(b)

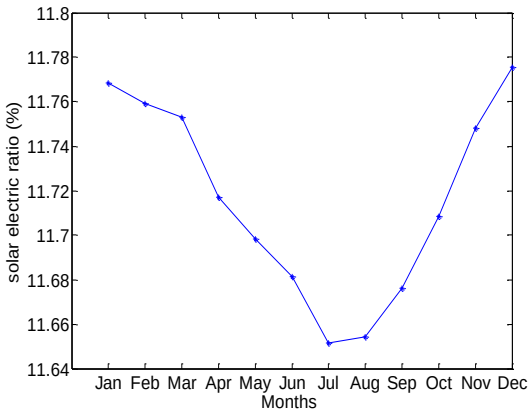

(c)

Figure 7. Effect of ambient temperature: a) ISCC power and efficiency; b) CC power and efficiency; c) Solar electrical ratio

Table 13. Average ambient temperatures during nights

Month	Jan	Feb	Mar	Apr	May	Jun	Jul	Aug	Sep	Oct	Nov	Dec
T (°C)	3.7	4.8	6.4	11.7	16.8	19.6	25.1	25.0	21.5	14.0	8.9	2.3

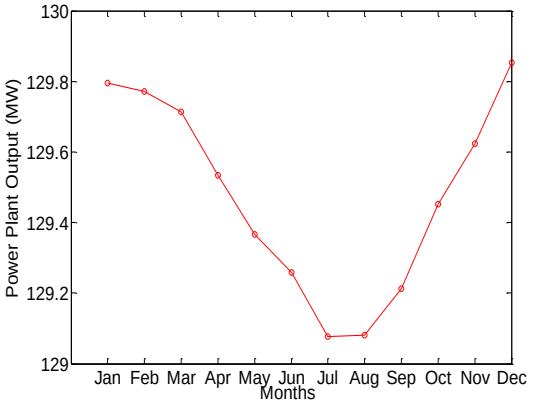

(a)

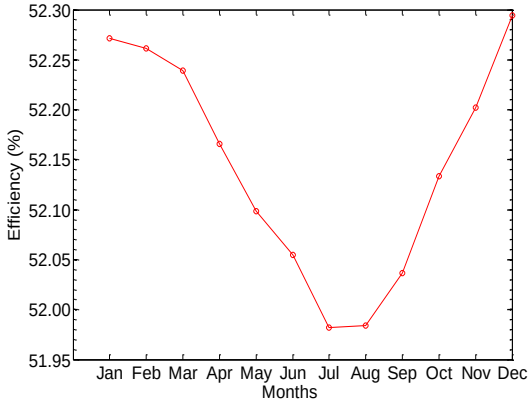

(b)

Figure 8. Performance of ISCC during nights and cloudy days: a) Power; b) Efficiency

Received:Added at production | Revised:Added at production | Accepted: Added at production
DOI: xxx/xxxx

Table 14 compares between the three power plants in terms of LCOE, fuel saving and emission, considering CC as the reference power plant. Fig. 9 and Fig.10 show the calculated LCOE subdivided into three parts: investment cost, O&M cost and fuel cost. LCOE is greatly affected by the specific cost of power plant, especially the solar parts, since their costs are very high compared to the fossil parts. According to Fig. 9 when the environmental cost is not taken into consideration, CC power plant has the lowest LCOE followed by GT. In the case of ISCC, LCOE has a value higher by 3 % compared with GT and 28 % higher than CC. If one considers the environmental effects as shown by Fig. 10, LCOE of ISCC becomes 0.0272 $/kWh which is about 6 % lower than for GT and 20 % higher than CC, but LCOE of CC is still the lowest. Fig. 11 and Fig. 12 show the specific fuel consumption (kg/MWh) and CO_2 emission (kg/MWh). ISCC has the lowest specific fuel consumption about 7 % which is lower than that of CC and 32 % lower than GT. As a consequence, ISCC allows saving about 18.45 million $ of fuel consumption through 30 years of its operation. Fig. 12 permits concluding that CO_2 emission is proportional to the fuel consumed, which is extremely high in TG but lesser in CC power plant. Due to availability of the solar energy during the day, ISCC has the lowest CO_2 emission, thus avoiding 0.89 million ton of CO_2 emission over 30 years of its operational period.

Table 14. Estimated LCOE

Parameter	GT	CC	ISCC
DNI per year (kWh/m$_2$ yr)	-	-	1999.38
Annual electricity production (MWh)	658752	909228	972896.8
LCOE $_a$ ($/kWh)	0.0216	0.0174	0.0222
LCOE $_b$ ($/kWh	0.0289	0.0227	0.0272
Fuel saving in 30 years (Million $)	-	-	18.45
Avoided CO_2 emission in 30 years (Million Ton)	-	-	0.89

$_a$ Without considering environmental cost
$_b$ With considering environmental cost

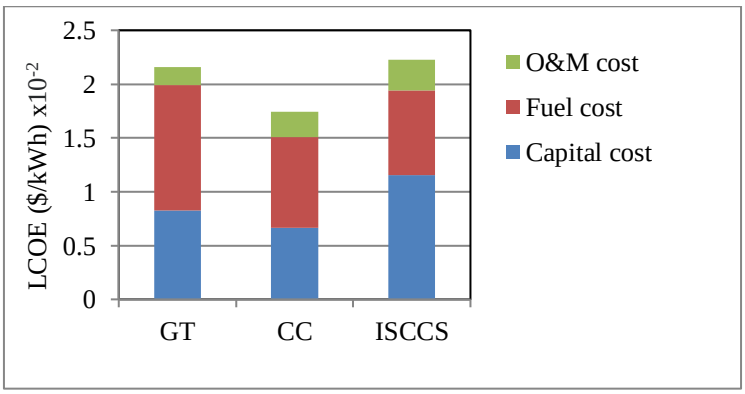

Figure 9. LCOE of different power plants without environmental cost

Received:Added at production | Revised:Added at production | Accepted: Added at production
DOI: xxx/xxxx

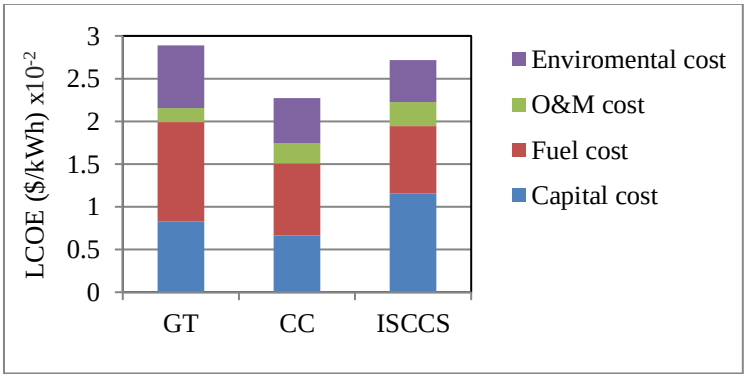

Figure 10. LCOE of different power plants by considering environmental cost

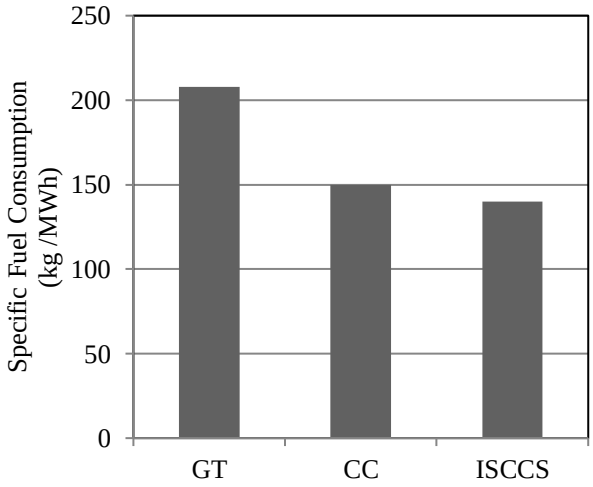

Figure 11. Specific consumption of natural gas

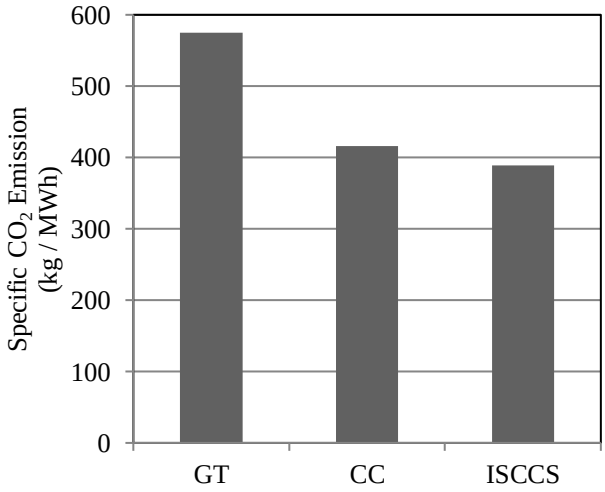

Figure 12. CO_2 emission of different power plants

6 | CONCLUSION

ISCCS plant coupled with PTC has shown that during daytime the solar energy could be converted at a solar electricity ratio about 17 % while the plant thermal efficiency may reach more than 63 % which is higher than in CC. On the other hand, when considering the

Received:Added at production | Revised:Added at production | Accepted: Added at production
DOI: xxx/xxxx

environmental cost, LCOE of ISCC is equal to 0.0272 $/kWh which is about 20 % higher than CC. The annual solar contribution of ISCC results in fuel consumption about 140 kg/MWh which is about 7 % lower than CC, but allows saving about 18.45 million $ of fuel through 30 years of operation. Moreover, CO_2 emission is lowered by reducing 0.89 million ton rejected over 30 years. The integration of fossil fuel – natural gas with solar energy for the replacement of the latent heat by using HSSG in parallel with HRSG is a very attractive option to make the transition from simple the GT and CC to the ISCC power plants. The results obtained concur well the feasibility and benefits of integrating the solar technology. Despite the current costs of PTC parts, it seems that their integration of CRS could be a promising option to be considered in the Algerian program aimed to produce 22000 MWe from the renewable energy.

DECLARATION OF CONFLICTING INTERESTS

The author(s) declared no potential conflicts of interest with respect to the research, authorship and/or publication of this article.

FUNDING

The author(s) received no financial support for the research, authorship and/or publication of this article.

ORCID

Adel-Ghenaiet: https://orcid.org/0000-0001-5112-3551

NOTATIONS

A	Heat exchanger surface area [m_2]
A_{abs}	Outer area of the absorber [m2]
A_c	Collector aperture area [m2]
APP	Approach point[°C]
C	Capital cost [$]
Cc	Concentration ratio
C_{pa}	Specific heat of the air in the compressor section
$\bar{C}_{pg}$	Mean specific heat of the exhaust gases in the HRSG [J/kg.K]
C_{pHTF}	Heat capacity of the Heat transfer fluid HTF [kJ/kg.K]
DNI	Direct normal irradiation [W/m_2]
F	Correction factor
h	Enthalpy [kJ/kg]
h_s	Steam enthalpy [kJ/kg]
h_w	Water enthalpy [kJ/kg]
$LCOE$	Levelized cost of energy [$/kWh]
f	fuel by air ratio
$\dot{m}_a$	Air mass flow [kg/s]
$\dot{m}_f$	Fuel mass flow [kg/s]
$\dot{m}_g$	Mass gas flow [kg/s]
$\dot{m}_s$	Steam mass flow [kg/s]
$\dot{m}_{SF}$	HTF mass flow rate [kg/s]
N_L	Number of line in the solar field
P_a	Atmospheric pressure [bar]

Received:Added at production | Revised:Added at production | Accepted: Added at production
DOI: xxx/xxxx

pp	Pinch point [°C]
Q	Heat exchanger duty [W]
Q_a	Assumed duty [W]
Q_{PTC}	Useful energy gained by the collector per unit of time [MW]
L_{cv}	Natural gas calorific value [kJ/kg]
Q_{SF}	Total useful energy gained in the SF per unit of time [MW]
P_{FP}	Pressure feed pump
P_{SPT}	Steam turbine output [MW]
P_{GT}	Gas turbine output [MW]
sfc	specific fuel consumption of the gas turbine [kJ/kg]
ST	Solar time [hour]
T	Temperature [K]
T_a	Ambient temperature [°C]
T_{abs}	Mean absorber pipe temperature [°C]
T_s	Steam temperature [°C]
T_{sat}	Water saturation temperature [°C]
U	Overall heat transfer coefficient [W/m2 K]
UA	Product of U and surface area A [W/K]
U_{abs}	Absorber thermal loss coefficient [W/m2 K]
ΔTpp	Pinch point [°C]
ΔTap	Approach point [°C]
ΔT_{SF}	Temperature difference between inlet and outlet of HTF [°C]
ΔTLM	Logarithmic mean temperature difference [°C]

Greek symbols

α	Absorptivity (%)
γ	Intercept factor
η_{SF}	Solar efficiency
η_{cc}	Combustion efficiency
η_e	Electrical efficiency
η_{ISCC}	Efficiency of the plant
η_m	Mechanical efficiency
$\eta_{optique}$	Optical efficiency
η_p	Pump efficiency
θ	Angle of incidence [deg]
θ_z	Zenith angle [deg]
ρ	Reflectivity
τ	Transmissivity
τ_b	Atmospheric transmittance
ϕ	Latitude [deg]

Abbreviation

CC	Combined cycle
Eco	Economizer
Evap	Evaporator
GT	Gas Turbine
HRSG	Heat Recovery Steam Generation
HSSG	Heat Solar Steam Generation
HTF	Heat Transfer Fluid
IN/ OUT	Inlet / Outlet
LCOE	Electricity production and levelized electricity cost
ISCC	Integrated Solar Combined Cycle
PF	Feed pump
PTC	Parabolic Trough Collector
Sh	Superheater
s	Steam

Received:Added at production | Revised:Added at production | Accepted: Added at production
DOI: xxx/xxxx

w Water

REFERENCES

[1] Goswami DY., Kreith F.; 2007 . Energy conversion. Taylor & Francis Group, USA, 2007.

[2] Zachary J.; 2013. Integrated solar combined cycle (ISCC) systems. Bechtel Corp, USA, 2013.

[3] Zhu G, Neises T,Turchi C, Bedilion R. Thermodynamic evaluation of solar integration into a natural gas combined cycle power plant. Renewable Energy 2015; 74:815-824. doi.org/10.1016/j.renene.2014.08.073

[4] Turchi CS, Ma Z. Co-located gas turbine/solar thermal hybrid designs for power production. Renewable energy 2014; 64:172-179.doi.org/10.1016/j.renene.2013.11.005

[5] Price H, Kearney K, Parabolic-Trough Technology Roadmap: A Pathway for Sustained Commercial Development and Deployment of Parabolic-Trough Technology. USA: Roadmap Workshop Participants; 1998.

[6] Okoroigwe E, Madhlopa A. An integrated combined cycle system driven by a solar tower: A review.Renewable and Sustainable Energy Reviews 2016; 57:337–350.http://dx.doi.org/10.1016/j.rser.2015.12.092.

[7] Nezammahalleh H, Farhadi F, Tanhaemami M.; 2010. Conceptual design and techno-economic assessment of integrated solar combined cycle system with DSG technology. Solar Energy 84 (2010) 1696–1705. DOI:10.1016/j.solener.2010.05.007.

[8] Rovira A, Montes MJ, Varela F, Gil M.; 2013. Comparison of heat transfer fluid and direct steam generation technologies for integrated solar combined cycles. Applied Thermal Engineering (2013) 264-274. DOI: 10.1016/j.applthermaleng.2012.12.008.

[9] Franchini G, Perdichizzi A, Ravelli S, Barigozzi G. ; 2013. A comparative study between parabolic trough and solar tower technologies in Solar Rankine Cycle and Integrated Solar Combined Cycle plants. Solar Energy 98 (2013) 302-314. doi.org/10.1016/j.solener.2013.09.033.

[10] Abdel-Dayem AM, Metwally MN, Alghamdi AS, Marzouk EM.; 2014. Numerical simulation and experimental validation of integrated solar combined power plant. Energy Procedia 50 (2014) 290 – 305. DOI: 10.1016/j.egypro.2014.06.036.

[11] Aldali Y, Morad K.; 2016. Numerical simulation of the integrated solar/North Benghazi combined power plant. (2016) Applied Thermal Engineering 108 (2016) 785–792. doi.org/10.1016/j.applthermaleng.2016.07.178.

[12] Dersch J, Geyer M, Geyer M, Herrmann U, Jones SA, Kelly B, Kistner R, Ortmanns W, Pitz-Paal R, Price H.; 2004. Trough integration into power plants-a study on the performance and economy of integrated solar combined cycle systems. Energy 29 (2004) 947–959. Doi:10.1016/S0360-5442(03)00199-3

[13] Montes MJ, Rovira A, Muñoz M, Martínez-Val JM.; 2011. Performance analysis of an integrated solar combined cycle using direct steam generation in parabolic trough collectors, Applied Energy 88 (2011) 3228–3238. doi:10.1016/j.apenergy.2011.03.038.

[14] Antonanzas J, Jimenez E, Blanco J, Antonanzas-Torres F.; 2014. Potential solar thermal integration in Spanish combined cycle gas turbines, Renewable and Sustainable Energy Reviews 37(2014)36–46. doi.org/10.1016/j.rser.2014.05.006.

[15] Price H, Kearney D.; 2003. Reducing the cost of energy from parabolic trough solar power plants, National Renewable Energy Laboratory, NREL/CP-550-33208, USA, January 2003.

Received:Added at production | Revised:Added at production | Accepted: Added at production
DOI: xxx/xxxx

[16] Horn M, Fuhring H, Rheinlander J.; 2004. Economic analysis of integrated solar combined cycle power plants. Energy 29 (2004) 935–945. Doi: 10.1016/S0360-5442(03)00198-1.

[17] Hosseini R, Soltani M, Valizadeh G.; 2005. Technical and economic assessment of the integrated solar combined cycle power plants in Iran. Renewable Energy 30 (2005) 1541–1555. DOI:10.1016/j.renene.2004.11.005.

[18] Mokheimer EMA, Dabwan Y N, Habib M A. ; 2015. Optimal integration of solar energy with fossil fuel gas turbine cogeneration plants using three different CSP technologies in Saudi Arabia. Journal of Applied Energy (2015), Volume 185, Part 2, 1, Pages 1268-1280.

[19] Duan L, Qu W, Jia S, Feng T.; 2017. Study on the integration characteristics of a novel integrated solar combined cycle system. Energy 130 (2017) 351–364, http://dx.doi.org/10.1016/j.energy.2017.04.118.

[20] Li Y, Xiong Y.; 2018. Thermo-economic analysis of a novel cascade integrated solar combined cycle system, Energy 145 (2018) 116–127, https://doi.org/10.1016/j.energy.2017.12.128.

[21] [21] Price H, Lüpfert E, Kearney D, Zarza E, Cohen G, Gee R, Mahoney R.; 2002. Advances in parabolic trough solar power plants, Journal of Solar Energy Engineering 124 (2002) 109-125. Doi:10.1115/1.1467922.

[22] Gueymard CA. A review of validation methodologies and statistical performance indicators for modeled solar radiation data: Towards a better bankability of solar projects. Renew Sustain Energy Rev 2014; 39:1024–34.

[23] Duffie AJ, Beckman AW. Solar engineering of thermal processes.2nd edition.New York: Wiley; 1991.

[24] Wong LT, Chow WK. Solar radiation model. Appl Energy 2001; 69:191–224.

[25] Geuymard CA. Direct solar transmittance and irradiance predictions with broadband models. Part I: detailed theoretical performance assessment. Solar Energy 2003;74:381–95.

[26] ASHRAE. Handbook of HVAC Applications. ASHRAE, Atlanta; 2007

[27] Geuymard CA. Direct solar transmittance and irradiance predictions with broadband models. Part II: validation with high-quality measurements. Solar Energy 2003;74:355–79.

[28] Gueymard CA. Clear-sky irradiance predictions for solar resource mapping and large-scale applications: Improved validation methodology and detailed performance analysis of 18 broadband radiative models. Solar Energy 2012; 86:2145–69.

[29] Zarza Romero-Alvarez M.; 2007. Concentrating solar thermal Power. Chap 21, Plataforma Solar de Almeria-CIEMAT: Taylor & Francis Group; 2007

[30] ISCC Hassi-R'mel power plant. 2014, Operating manual 2014.

[31] Cohen GE, Kearny DW, Gregory JK.; 1999. Final report on the operation and maintenance improvement program for concentrating solar power plants, 1999, SAND 99-1290.

[32] National meteorological Office (ONM). 2014, Report (2014) Algeria.

[33] Horlock JH. Advanced gas turbine cycles. UK: Elsevier Science Ltd; 2003.

[34] Razak AMY. Industrial gas turbines 'Performance and operability'. USA: Taylor & Francis Group; 2007.

[35] Kim TS, Ro ST. Comparative evaluation of the effect of turbine configuration on the performance of heavy-duty gas turbines. ASME 1995;95-GT-334:V004T10A019. Doi:10.1115/95-GT-334.

Received:Added at production | Revised:Added at production | Accepted: Added at production
DOI: xxx/xxxx

[36] Wilcox M, Baldwin R, Garcia-Hernandez A, Brun K. Guideline for gas turbine inlet air filtration systems. USA: Gas Machinery Research Council Southwest Research Institute; 2010.

[37] Çengel AY. Introduction to Thermodynamics and Heat Transfer.2nd edition. USA: McGraw−Hill Primi; 2008.

[38] Wilcock R.C, Young J.B, Horlock J.H, 2005.The effect of turbine blade cooling on the cycle efficiency of gas turbine power cycles. Journal of Engineering for Gas turbines and Power 127(1) (2005) 109–120.

[39] Ganapathy V.; 2003. Industrial boilers and heat recovery steam generators, Marcel Dekker, USA, 2003.

[40] Ganapathy V.; 2015. Steam generators and waste heat boilers for process and plant engineers, Taylor & Francis Group, USA, 2015.

[41] U.S. Energy Information Administration: Jun 25, 2019, https://www.eia.gov/naturalgas/monthly/pdf/table_03.pdf